

# EduVQA: Benchmarking AI-Generated Video Quality Assessment for Education

Baoliang Chen Xinlong Bu Lingyu Zhu Hanwei Zhu Xiangjie Sui

## Abstract

While AI-generated content (AIGC) models have achieved remarkable success in generating photorealistic videos, their potential to support *visual, story-driven learning in education* remains largely untapped. To close this gap, we present **EduAIGV-1k**, the **first benchmark dataset and evaluation framework** dedicated to assessing the quality of AI-generated videos (AIGVs) designed to teach foundational math concepts, such as numbers and geometry, to young learners. EduAIGV-1k contains 1,130 short videos produced by ten state-of-the-art text-to-video (T2V) models using 113 pedagogy-oriented prompts. Each video is accompanied by **rich, fine-grained annotations** along two complementary axes: (1) **Perceptual quality**, disentangled into **spatial and temporal fidelity**, and (2) **Prompt alignment**, labeled at the **word-level** and **sentence-level** to quantify the degree to which each mathematical concept in the prompt is accurately grounded in the generated video. These fine-grained annotations transform each video into a multi-dimensional, interpretable supervision signal, far beyond a single quality score. Leveraging this dense feedback, we introduce **EduVQA** for both perceptual and alignment quality assessment of AIGVs. In particular, we propose a Structured 2D Mixture-of-Experts (**S2D-MoE**) module, which enhances the dependency between overall quality and each sub-dimension by shared experts and dynamic 2D gating matrix. Extensive experiments show our EduVQA consistently outperforms existing VQA baselines. Both our dataset and code will be publicly available.

## 1. Introduction

The recent rise of text-to-video (T2V) generation models (Li et al., 2018; Hong et al., 2022; OpenAI, 2024; Kling AI, 2024) has opened new possibilities for scalable, visual storytelling content creation. These advancements hold particular promise for technology-assisted education, where richly animated, concept-driven videos could offer young

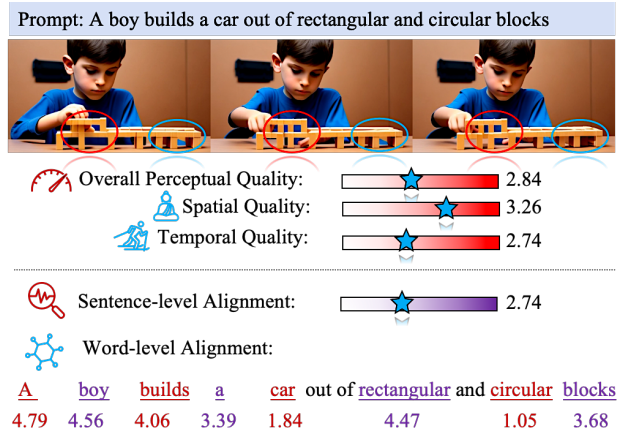


Figure 1. Annotation structure of our constructed EduAIGV-1k dataset. Each educational video is annotated with spatial and temporal fidelity and word-level semantic consistency, enabling a fine-grained assessment of perceptual quality and prompt alignment. The red and blue elliptical regions indicate temporal inconsistencies that negatively impact temporal quality.

learners intuitive explanations of abstract ideas. However, despite the impressive visual quality of modern AIGC models, their application in instructional video generation for early education remains largely underexplored and critically under-evaluated.

We argue that evaluating the quality of AI-generated videos (AIGVs) in educational contexts presents new and unique challenges. Beyond general perceptual quality, such as spatial clarity or temporal smoothness, educational videos must faithfully convey the intended instructional content. For example, when asked to illustrate “three blue blocks”, a generated video that is aesthetically pleasing but lacks correct semantic grounding fails to serve its pedagogical purpose. Unfortunately, existing AIGV benchmarks primarily focus on entertainment, realism, or general coherence (Chen et al., 2024; Kou et al., 2024b), providing limited support for fine-grained content or instruction-aligned evaluation.

To fill this gap, we introduce EduAIGV-1k, the first benchmark dataset and evaluation framework for assessing the quality of AIGVs intended for early math education. The dataset consists of 1,130 videos generated by ten state-of-the-art T2V models using 113 expert-curated prompts, covering core math concepts, including numbers, geometry, measurement, and probability. More importantly, we move

beyond global scoring by providing rich, fine-grained annotations along two complementary dimensions: **(1) Perceptual quality**, decomposed into spatial and temporal fidelity; **(2) Prompt alignment**, annotated at the word level to quantify semantic correctness. An overview of our annotation structure is shown in Fig. 1.

To fully exploit the fine-grained supervision provided by EduAIGV-1k, we propose **EduVQA**, a dual-path framework designed for both perceptual quality and prompt alignment assessment of AIGVs. At its core lies the **Structured 2D Mixture-of-Experts (S2D-MoE)** module, which explicitly models the hierarchical dependencies between overall and sub-dimension qualities in each path. Specifically, S2D-MoE introduces a shared expert pool that enforces representation coherence across related sub-dimensions, while its 2D gating mechanism adaptively models the interactions between different sub-tasks. Compared to conventional 1D MoE, this structured weighting scheme ensures that overall quality inference is guided by the collective knowledge of sub-dimensions, thereby enhancing model interpretability and generalization. Our contributions are listed as follows:

- We propose the first benchmark for evaluating AIGV quality in early math education, including 1,130 videos generated from 113 expert-curated prompts.
- We introduce a rich, fine-grained annotation scheme that supervises spatial, temporal, and both word- and sentence-level alignment quality, enabling more precise and structured evaluation.
- We propose EduVQA, a unified framework for assessing the quality of AIGVs. Its core S2D-MoE module explicitly models hierarchical dependencies between overall and sub-dimensional qualities via shared experts and a 2D gating matrix.
- Comprehensive experiments demonstrate that EduVQA substantially outperforms existing VQA models and maintains superior performance on unseen AIGVQA datasets, highlighting its strong effectiveness and generalization capability.

## 2. Related Work

### 2.1. Video Generation Models

T2V generation has rapidly evolved through three architectural paradigms. VAE/GAN-based models (Li et al., 2018; Deng et al., 2019) extend image VAEs and GANs by adding temporal modules (e.g., 3D convolutions or recurrent layers) to synthesize short clips. While capable of fast sampling, these approaches often suffer from mode collapse and limited motion coherence. Autoregressive models treat frame generation as a sequence prediction task, leveraging transformer architectures to predict pixels or latent tokens one step at a time (Wu et al., 2022a; Hong et al., 2022;

Wang et al., 2024b). This yields improved fidelity but tends to accumulate errors and exhibit temporal drift over long horizons. Diffusion models have recently become dominant, generating videos by iteratively denoising noise conditioned on spatial-temporal context (Ho et al., 2022; Chen et al., 2023b; Esser et al., 2023; OpenAI, 2024; Kling AI, 2024). By refining all frames jointly at each step, diffusion methods avoid adversarial instability and deliver superior global consistency. Despite these advances, existing T2V models still struggle with content fidelity and text-video alignment, underscoring the need for dedicated AIGVQA supervision to guide quality-aware video generation.

### 2.2. Quality Metrics for AIGC Videos

Assessing AIGVs requires metrics that capture both perceptual quality (spatial and temporal fidelity) and prompt alignment (semantic correctness). Early evaluations borrowed image-centric metrics like Inception Score (IS) (Salimans et al., 2016) and Fréchet Inception Distance (FID) (Heusel et al., 2017) alongside classical IQA measures (e.g., NIQE (Mittal et al., 2012)) and learned predictors (e.g., MUSIQ (Ke et al., 2021)). However, these frame-level approaches ignore temporal artifacts and only loosely correlate with human judgments. Video-level extensions such as Fréchet Video Distance (FVD) (Unterthiner et al., 2018) and UGC-focused VQA models (e.g., VSFA (Li et al., 2019), FastVQA (Wu et al., 2022b)) incorporate motion consistency but remain trained on natural videos, limiting their sensitivity to AIGC-specific distortions. For semantic alignment, most methods employ CLIP-based similarity by averaging frame-wise text-image scores (Radford et al., 2021), which overlooks concept order and dynamic content. Benchmarks like EvalCrafter (Liu et al., 2024) and VBench (Huang et al., 2024) propose multiple objective metrics, yet still lack fine-grained evaluation for domains such as educational video generation.

## 3. EduAIGV-1K: Fine-Grained Video Quality Evaluation in Math Education

### 3.1. Data Collection

Our EduAIGV-1K dataset is constructed to facilitate fine-grained evaluation of AIGVs in the context of mathematics education, with a particular emphasis on young learners. Although recent T2V models have achieved remarkable progress, they still struggle to render highly *abstract*, *symbolic*, or *spatially precise* concepts. For instance, most models fail to accurately depict complex numerosity (e.g., “fifteen children dancing in a circle”) or detailed geometric transformations (e.g., “a triangle rotating 90 degrees clockwise around its vertex”). Such precise object counting and subtle motion representation remain beyond the current ca-



Figure 2. An overview of our dataset, divided into four categories: *Numbers*, *Geometry*, *Measurement*, and *Probability*.

pabilities of T2V models. Given these limitations, although our long-term goal is to support a broad range of mathematical content, the initial version of our dataset is intentionally focused on visually realizable concepts that current T2V models can reasonably depict. These concepts, in turn, are particularly well-suited for young learners, who benefit most from the visual grounding of abstract ideas.

**Prompt Design.** To guarantee pedagogical relevance, we derive prompt content from widely recognized educational standards: the *TIMSS 2023 Assessment Frameworks* (Mullis et al., 2021) and the *Common Core State Standards for Mathematics* (CCSSI, United States (Core, 2010)). Based on these sources, we identify four domains where current T2V capabilities are most applicable: *Numbers*, *Geometry*, *Measurement*, and *Probability*. We leverage GPT-4o to generate candidate prompts by grounding curriculum-relevant concepts in concrete, visually plausible everyday scenarios, bridging the gap between abstract mathematical ideas and T2V generation capability. From an initial pool, we curate 113 high-quality prompts via expert filtering, covering four core domains in early mathematics education: *Numbers* (43 prompts), *Geometry* (40 prompts), *Measurement* (20 prompts), and *Probability* (10 prompts), ensuring topical diversity. Each domain encompasses several pedagogically meaningful subtypes to balance conceptual breadth and visual renderability. Specifically, the *Numbers* domain spans key concepts such as *counting*, *number comparison*, *basic number operations*, and *basic fractions*; *Geometry* includes *shape recognition*, *shape composition*, *spatial reasoning*, and *reasoning about attributes*; *Measurement* focuses on *measurable attributes and categorical data*; and *Probability* introduces *foundational ideas of randomness and chance*, which are essential for early probabilistic thinking. Example

videos across the four topics are visualized in Fig. 2.

**T2V Model Selection.** To ensure diversity and representativeness in the generated content, we employ ten widely-used T2V models, encompassing both open-source and commercial systems. The selected models include: *CogVideo* (Hong et al., 2022), *Gen-3* (Runway Research, 2024), *Hotshot-XL* (Mullan et al., 2023), *Dreamina* (ByteDance, 2024), *Kling* (Kling AI, 2024), *La Vie* (Wang et al., 2024a), *LVDM* (He et al., 2022), *Show-1* (Zhang et al., 2025), *Text2Video-Zero* (Khachatryan et al., 2023), and *VideoCrafter* (Chen et al., 2023a). These models vary in terms of frame rate, resolution, duration, and motion quality, providing a robust sampling of T2V generation characteristics. For instance, *Kling* produces the highest frame rate (30 FPS), while *Dreamina* achieves the highest spatial resolution (1472×832). In contrast, *LVDM* and *Text2Video-Zero* yield the lowest resolution (256×256) and frame rate (4 FPS), respectively. Regarding duration, *CogVideo* generates the longest clips (up to 6 seconds), while *Hotshot-XL* and *VideoCrafter* produce shorter sequences (around 1 second). In total, we generate 1,130 videos across the 113 prompts, with multiple models applied per prompt.

### 3.2. Human Feedback Consolidation

To enable precise evaluation of the collected AIGVs, each video in the *EduAIGV-1K* dataset is annotated along two main dimensions:

*Perceptual Quality.* This dimension characterizes video visual fidelity from three complementary perspectives:

- *Spatial Quality:* evaluates frame-level fidelity through texture clarity, edge sharpness, and artifact absence.
- *Temporal Quality:* assesses motion coherence across

frames, considering smoothness and temporal stability.

- *Overall Perceptual Quality*: reflects a holistic impression integrating spatial and temporal aspects.

*Prompt Alignment*. This dimension measures the semantic consistency between the textual prompt and the generated video content:

- *Word-Level Alignment*: examines whether individual keywords or visual entities specified in the prompt are accurately represented in the video.
- *Sentence-Level (Overall) Alignment*: evaluates how well the overall visual semantics correspond to the intended meaning of the prompt.

A total of 19 trained annotators participated in the labeling process. Before annotation, all participants completed a structured training session using a held-out set of videos to calibrate their perception of visual distortions and semantic alignment. The annotation procedure followed the ITU-R BT.500 recommendations for subjective VQA. Each video was independently rated across all five dimensions using a 5-point Likert scale (1: very poor, 5: excellent), ensuring comprehensive and unbiased human evaluation across both perceptual and semantic aspects.

After collecting raw ratings from all participants, we perform outlier removal at the individual rating level to ensure annotation quality and consistency. For each video-dimension pair, given a set of scores  $\{x_i\}_{i=1}^N$ , we compute the sample mean  $\mu$  and standard deviation  $\sigma$ , and define the inlier set as

$$\mathcal{I}_{\text{inlier}} = \{i \mid |x_i - \mu| \leq \lambda \cdot \sigma\}, \quad (1)$$

where the threshold  $\lambda$  is set to 2.0 for approximately Gaussian-distributed dimensions, and to  $\sqrt{20}$  for dimensions exhibiting significant deviations from normality. Ratings falling outside  $\mathcal{I}_{\text{inlier}}$  are excluded from aggregation. Furthermore, annotators with more than 5% of their ratings identified as outliers across all evaluations are removed from subsequent analysis. Annotators are retrained with additional guidance and example-based calibration before returning to the annotation pipeline. More details regarding our dataset construction can be found in the supplementary.

### 3.3. Annotation Processing and Analysis

The distributions of MOS across the five quality dimensions are shown in Fig. 3(a)-(e). In particular, the *Spatial Quality*, *Overall Perceptual Quality*, and *Sentence-Level Prompt Alignment* dimensions exhibit approximately Gaussian distributions centered around moderate values, suggesting consistent perceptual fidelity and general semantic correspondence in the majority of videos. By contrast, the *Temporal Quality* shows a distinctly bimodal distribution, reflecting the dual nature of model behavior: either producing

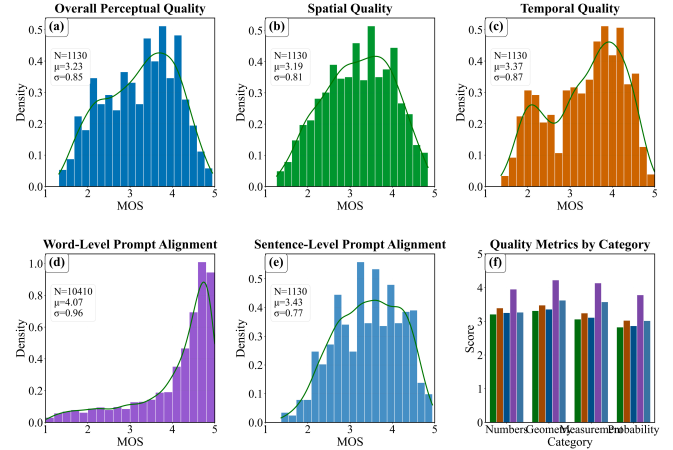


Figure 3. Annotation Analysis. (a)-(e): MOS distributions across five dimensions; (f): Average MOS of each scene category.

temporally stable but static scenes or attempting complex motion that often results in temporal artifacts and lower scores. The *Word-Level Prompt Alignment* dimension is skewed toward higher scores but retains a heavy tail toward lower values. This indicates that while many key terms are visually grounded, certain abstract remain difficult for current T2V models to represent accurately. The average MOS for each scene category is shown in Fig. 3(f).

## 4. EduVQA: Multi-dimensional Quality Assessment for AIGV

### 4.1. Overview

As illustrated in Fig. 4, our proposed EduVQA aims to provide fine-grained and interpretable VQA for AIGVs, jointly predicting *perceptual quality* and *prompt alignment quality*. EduVQA adopts a dual-path architecture, where the perceptual path models low-level distortions (spatial and temporal), while the alignment path evaluates text-video correspondence at both word and sentence levels.

**Feature Extraction.** Given an input video  $\mathcal{V}$  and its corresponding prompt  $\mathcal{T}$ , our goal is to extract both perceptually sensitive and semantically aligned representations. Following T2VQA (Kou et al., 2024a), we employ a Video Swin Transformer (Liu et al., 2022) to extract video quality-sensitive features, and utilize BLIP (Li et al., 2022b) as a multimodal encoder to obtain fused visual-textual features:

$$F_{VST} = \Phi_{VST}(\mathcal{V}), \quad F_{VST} \in \mathbb{R}^{T \times H \times W \times C}, \quad (2)$$

$$F_{BLIP} = \Phi_{BLIP}(\mathcal{V}, \mathcal{T}), \quad F_{BLIP} \in \mathbb{R}^{T \times L \times C}, \quad (3)$$

where  $T$ ,  $H$ ,  $W$  denote the temporal and spatial dimensions, and  $L$  is the token length of the input text.

**Cross-modal interaction.** To aggregate multimodal semantics, two cross-attention operations are designed in op-

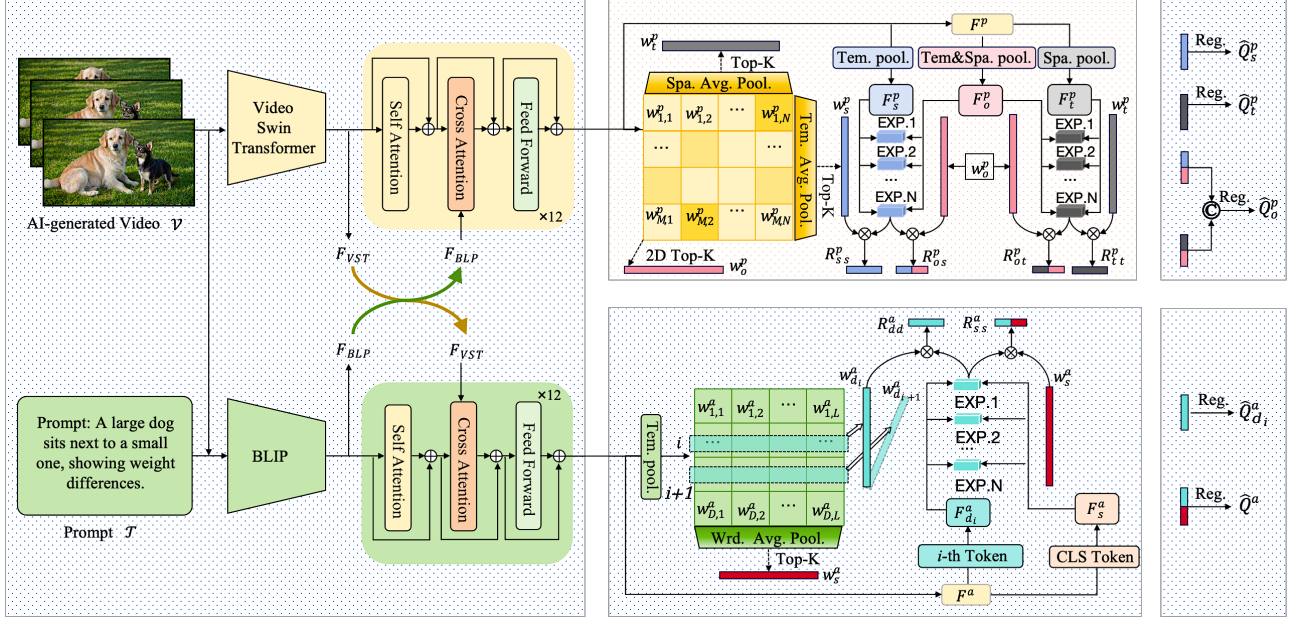


Figure 4. Overview of EduVQA framework. We jointly predict five quality dimensions via a dual-path framework equipped with 2D MoE.

posite directions. When generating perceptual-aware features  $F_p$ , we use  $F_{VST}$  as the *query* and  $F_{BLIP}$  as the *key*:

$$F_p = \text{CrossAttn}(F_{VST}, F_{BLIP}), \quad (4)$$

while for alignment features  $F_a$ , the direction is reversed:

$$F_a = \text{CrossAttn}(F_{BLIP}, F_{VST}). \quad (5)$$

**Philosophy of Structured 2D Mixture-of-Experts (S2D-MoE).** In the subsequent dual-path prediction stage, we incorporate S2D-MoE to capture and strengthen the hierarchical relationships between overall and sub-dimensional quality predictions within each path. Compared to conventional MoE layers that activate experts independently for each task, S2D-MoE introduces two key mechanisms: *expert sharing* and an *adaptive 2D gating matrix*.

The shared expert pool tightly couples the representation learning of the overall-quality with that of each sub-dimension by requiring them to rely on a common set of experts. This design ensures that the overall-quality representation is intrinsically grounded in features that remain sensitive to each sub-dimension, thereby preventing the overall predictor from diverging from the fine-grained quality semantics. Building upon this shared foundation, the adaptive 2D gating matrix further models the hierarchical dependence between tasks by integrating the sub-dimension-specific expert weights into the overall gating distribution. As a result, the overall prediction becomes an explicit aggregation of sub-dimension contributions. Collectively, these mechanisms establish a coherent representational structure in which overall quality inference is consistently aligned with

all sub-dimensions, ultimately improving interpretability and generalization in multi-dimensional quality assessment.

## 4.2. Perceptual Quality Path

Given perceptual features  $F_p \in \mathbb{R}^{T \times H \times W \times C}$ , our goal is to estimate spatial, temporal, and overall perceptual quality scores. We first generate a 2D adaptive gating matrix  $\mathbf{W}^p \in \mathbb{R}^{M \times N}$  from the  $F_p$ , representing the interaction importance between  $M$  spatial and  $N$  temporal experts.

**Structured expert activation.** We derive three sets of activation weights by pooling  $\mathbf{W}^p$ :

$$W_s^p = \text{TopK}(\text{Mean}_{\text{row}}(\mathbf{W}^p)), \quad (6)$$

$$W_t^p = \text{TopK}(\text{Mean}_{\text{col}}(\mathbf{W}^p)), \quad (7)$$

$$W_o^p = \text{TopK}(\mathbf{W}^p). \quad (8)$$

$W_s^p$  and  $W_t^p$  correspond to spatial and temporal gating weight, while  $W_o^p$  represents globally activated weights.

**Feature aggregation.** We perform average pooling along temporal and spatial dimensions on  $F_p$  to obtain:

$$F_s^p = \text{Pool}_T(F_p) \in \mathbb{R}^{H \times W \times C}, \quad (9)$$

$$F_t^p = \text{Pool}_{H,W}(F_p) \in \mathbb{R}^{T \times C}, \quad (10)$$

$$F_o^p = \text{Pool}_{T,H,W}(F_p) \in \mathbb{R}^C. \quad (11)$$

Each pooled feature is then processed by the corresponding

spatial and temporal expert sets  $\{E_j^s\}_1^M, \{E_j^t\}_1^N$ :

$$R_{ss}^p = \sum_{j=1}^M W_{s,j}^p E_j^s(F_s^p), \quad R_{tt}^p = \sum_{j=1}^N W_{t,j}^p E_j^t(F_t^p), \quad (12)$$

$$R_{os}^p = \sum_{j=1}^M W_{o,j}^p E_j^s(F_o^p), \quad R_{ot}^p = \sum_{j=1}^N W_{o,j}^p E_j^t(F_o^p). \quad (13)$$

**Quality regression.** After feature refinement, we obtain sub-quality and overall quality predictions as:

$$\hat{Q}_s^p = FC_s(R_{ss}^p), \quad (14)$$

$$\hat{Q}_t^p = FC_t(R_{tt}^p), \quad (15)$$

$$\hat{Q}_o^p = FC_o(R_{os}^p \oplus R_{ot}^p), \quad (16)$$

where  $FC$  denotes a fully connected layer, and ‘ $\oplus$ ’ represents concatenation along the channel dimension.

### 4.3. Prompt Alignment Path

The alignment branch operates on the multimodal representation  $F_a \in \mathbb{R}^{T \times D \times C}$ , where  $D$  denotes the number of textual tokens. Following the same philosophy of S2D-MoE, we compute an adaptive gating matrix  $\mathbf{W}^a \in \mathbb{R}^{D \times L}$ , where  $L$  represents the number of semantic experts.

**Token-wise and sentence-wise experts.** For each word token  $d_i$ , we obtain its expert weights:

$$W_{d_i}^a = \text{TopK}(\mathbf{W}^a[i, :]), \quad (17)$$

while sentence-level weights are derived by averaging across tokens:

$$W_s^a = \text{TopK}(\text{Mean}_i(\mathbf{W}^a[i, :])). \quad (18)$$

**Feature projection and regression.** We extract token-level and global textual features:

$$F_{d_i}^a = F_a[:, i, :], \quad F_s^a = F_a[:, \text{CLS}, :], \quad (19)$$

and process them via the alignment expert set  $\{E_j^a\}_1^Z$ :

$$R_{dd}^a = \sum_{j=1}^Z W_{d_i,j}^a E_j^a(F_{d_i}^a), \quad R_{ss}^a = \sum_{j=1}^Z W_{s,j}^a E_j^a(F_s^a), \quad (20)$$

leading to the final word-wise ( $\hat{Q}_{d_i}^a$ ) and sentence-wise ( $\hat{Q}_s^a$ ) alignment predictions:

$$\hat{Q}_{d_i}^a = FC_d(R_{dd}^a), \quad \hat{Q}_s^a = FC_s(R_{ss}^a). \quad (21)$$

### 4.4. Multi-task Optimization

The entire EduVQA is optimized under a multi-task objective  $\mathcal{L}_{\text{total}}$ :

$$\begin{aligned} \mathcal{L}_{\text{total}} = & \lambda_1 \mathcal{L}_{plcc}(\hat{Q}_s^p, Q_s^p) + \lambda_2 \mathcal{L}_{plcc}(\hat{Q}_t^p, Q_t^p) \\ & + \lambda_3 \mathcal{L}_{plcc}(\hat{Q}_o^p, Q_o^p) + \lambda_4 \frac{1}{L} \sum_{i=1}^L \mathcal{L}_{plcc}(\hat{Q}_{d_i}^a, Q_{d_i}^a) \\ & + \lambda_5 \mathcal{L}_{plcc}(\hat{Q}_s^a, Q_s^a), \end{aligned} \quad (22)$$

where  $\mathcal{L}_{plcc}$  denotes the Pearson Linear Correlation Coefficient loss (Wu et al., 2023a).  $Q_s^p, Q_t^p$ , and  $Q_o^p$  are the ground-truth spatial, temporal, and overall perceptual quality scores.  $Q_{d_i}^a$  and  $Q_s^a$  represent the ground-truth  $i$ -th word-level and sentence-level alignment quality, respectively.  $L$  is the number of word tokens, and  $\lambda_1$ – $\lambda_5$  balance the contributions of the sub-tasks. This joint optimization promotes interaction between sub-dimensional and overall predictions, enabling EduVQA to deliver accurate and interpretable prediction.

## 5. Experiments

### 5.1. Implementation details

We conduct experiments on the EduAIGV-1k dataset, which is split into training, validation, and test sets with a ratio of 6:2:2. To ensure fair comparison, we perform 10 random splits based on video categories and generative models. For each split, we ensure that the number of videos generated by each model and from each category is balanced. Final performance is reported as the average across these 10 splits. Each expert is implemented as a two-layer multilayer perceptron (MLP) with ReLU activation (Glorot et al., 2011). For each sub-dimension, we employ 8 experts ( $M=N=Z=8$ ) and all dimension select top-2 experts during routing. The model is optimized by the Adam optimizer (Kingma & Ba, 2014) with an initial learning rate of 1e-5. The  $\lambda_1$  to  $\lambda_5$  in Eqn. (22) are set by 0.125, 0.125, 0.25, 0.25, and 0.25, respectively. A cosine annealing schedule is used to gradually reduce the learning rate to zero over the course of training. We train the model for 50 epochs with a batch size of 4.

### 5.2. Baselines

To comprehensively benchmark our approach, we compare against a wide range of baselines across the two key quality dimensions: (1) *Perceptual Quality Baselines*. We evaluate several image and video quality assessment models. ImageReward (Xu et al., 2023), IPCE (Peng et al., 2024), and IP-IQA (Qu et al., 2024) are originally developed for image-level AIGC quality assessment. For video-oriented baselines, we consider DOVER (Wu et al., 2023b), BVQA (Li et al., 2022a), CLIPVQA (Xing et al., 2024), FasterVQA (Wu et al., 2023a), GSTVQA (Chen et al., 2021),

VSFA (Li et al., 2019), and SimpleVQA (Cheng et al., 2025), which are primarily designed for user-generated content (UGC) quality assessment. We fine-tune these models on our EduAIGV-1k dataset for fair comparison. Q-Align is evaluated in a zero-shot setting using publicly released weights. In addition, we include T2VQA, a recent method specifically designed for evaluating T2V generation models. (2) *Prompt Alignment Baselines*. We evaluate several vision-language models with strong zero-shot alignment capabilities, including CLIP (Wang et al., 2023), ImageReward (Xu et al., 2023), BLIP (Li et al., 2022b), and OpenVCLIP (Weng et al., 2023), using their pre-trained weights without fine-tuning. For image-based models, we aggregate the frame-wise results via average pooling.

Table 1. Comparison on *Perceptual Quality* and *Prompt Alignment* of EduAIGV-1k.  $\uparrow$ : higher is better,  $\downarrow$ : lower is better.

Metric	Setting	Method	SRCC $\uparrow$	PLCC $\uparrow$	KRCC $\uparrow$	RMSE $\downarrow$
Perceptual Quality	Zero-shot	ImageReward (Xu et al., 2023)	0.409	0.432	0.282	3.369
		Q-Align (Wu et al., 2023c)	0.644	0.669	–	–
	Fine-tuned	IPCE (Peng et al., 2024)	0.822	0.822	0.631	0.494
		IP-IQA (Qu et al., 2024)	0.852	0.863	0.666	0.434
		DOVER (Wu et al., 2023b)	0.832	0.840	0.645	0.479
		BVQA (Li et al., 2022a)	0.848	0.862	–	–
		CLIPVQA (Xing et al., 2024)	0.846	0.832	–	–
		FasterVQA (Wu et al., 2023a)	0.844	0.856	0.659	0.456
		GSTVQA (Chen et al., 2021)	0.837	0.849	0.655	0.456
		VSFA (Li et al., 2019)	0.803	0.805	0.611	0.515
		SimpleVQA (Cheng et al., 2025)	0.742	0.758	0.552	0.553
T2VQA (Kou et al., 2024a)	0.810	0.826	0.623	0.499		
<b>Ours</b>	<b>EduVQA</b>	<b>0.869</b>	<b>0.879</b>	<b>0.688</b>	<b>0.417</b>	
Prompt Alignment	Zero-shot	CLIP (Wang et al., 2023)	0.270	0.282	0.184	3.174
		ImageReward (Xu et al., 2023)	0.409	0.432	0.282	3.369
		BLIP (Li et al., 2022b)	0.457	0.392	0.317	101.113
		Open-VCLIP (Weng et al., 2023)	0.335	0.229	0.340	94.306
	Fine-tuned	IPCE (Peng et al., 2024)	0.634	0.643	0.460	0.604
		IP-IQA (Qu et al., 2024)	0.648	0.653	0.469	0.593
		T2VQA (Kou et al., 2024a)	0.731	0.733	0.544	0.564
		<b>Ours</b>	<b>EduVQA</b>	<b>0.757</b>	<b>0.768</b>	<b>0.571</b>

Table 2. Cross-dataset performance comparison. All models are trained on our EduAIGV-1k dataset.

Method	LGVQ Dataset			EvalCrafter Dataset	
	Spatial	Temporal	Alignment	Perceptual	Alignment
BVQA (Li et al., 2022a)	0.518 / 0.608	0.235 / 0.550	– / –	0.161 / 0.172	– / –
CLIPVQA (Xing et al., 2024)	0.509 / 0.480	0.355 / 0.287	– / –	0.319 / 0.325	– / –
FasterVQA (Wu et al., 2023a)	0.511 / 0.539	0.380 / 0.427	– / –	0.378 / 0.359	– / –
GSTVQA (Chen et al., 2021)	0.507 / 0.555	0.459 / 0.529	– / –	0.276 / 0.281	– / –
VSFA (Li et al., 2019)	0.498 / 0.516	0.174 / 0.246	– / –	0.213 / 0.195	– / –
SimpleVQA (Cheng et al., 2025)	0.395 / 0.442	0.262 / 0.394	– / –	0.268 / 0.289	– / –
IPCE (Peng et al., 2024)	0.324 / 0.336	0.428 / 0.473	0.201 / 0.190	0.247 / 0.255	0.245 / 0.253
IP-IQA (Qu et al., 2024)	0.423 / 0.473	0.363 / 0.454	0.267 / 0.256	0.242 / 0.239	0.131 / 0.137
T2VQA (Kou et al., 2024a)	0.466 / 0.504	0.402 / 0.453	0.521 / 0.539	0.305 / 0.299	0.553 / 0.554
<b>EduVQA (Ours)</b>	<b>0.536 / 0.593</b>	<b>0.511 / 0.571</b>	<b>0.529 / 0.547</b>	<b>0.408 / 0.398</b>	<b>0.586 / 0.599</b>

### 5.3. Quantitative Analysis

In Tab. 1, we present a comprehensive comparison across all baseline methods on the EduAIGV-1k dataset. Our proposed model, *EduVQA*, consistently outperforms existing methods in both perceptual quality and prompt alignment evaluation, demonstrating strong generalization capability for educational AIGC content. For perceptual quality evaluation, *EduVQA* achieves the best performance across all metrics, outperforming the state-of-the-art image-level model *IP-IQA* by +2.00% (SRCC), and +1.85% (PLCC). Notably, unlike image-based models such as *IP-IQA*, which process each frame independently, failing to capture temporal dynamics,

our video-level framework inherently models temporal dependencies. Compared to the strongest video-level baseline *BVQA*, *EduVQA* also shows consistent improvements of +2.48% in SRCC. In terms of prompt alignment, *EduVQA* significantly outperforms the most competitive fine-tuned model, *T2VQA*, achieving a +3.56% SRCC, and +4.77% PLCC improvement. These results highlight the superior capability of our *EduVQA* in modeling fine-grained video-text alignment beyond static frame-level correlations. In contrast, zero-shot models such as CLIP, BLIP, and ImageReward perform worse, further emphasizing the importance of domain adaptation for this task.

### 5.4. Cross-dataset Evaluation

To evaluate the generalization capability of our *EduVQA*, we conduct cross-dataset testing as shown in Tab. 2. All methods are trained on EduAIGV-1k dataset and directly tested on two unseen AIGVQA benchmarks, LGVQ (Zhang et al., 2024) and EvalCrafter (Liu et al., 2024), without any fine-tuning. Our model consistently surpasses existing approaches. On LGVQ, it achieves the highest SRCC in both spatial and temporal dimensions (0.536 and 0.511), demonstrating strong robustness to domain shift. It also establishes new state-of-the-art results in prompt alignment, confirming its superior understanding of text-conditioned semantics. When transferred to EvalCrafter, our model maintains leading performance in both quality dimensions. These results validate both the representational strength of EduAIGV-1k and the robustness of our model design.

### 5.5. Qualitative Examples

To further demonstrate the effectiveness of *EduVQA*, we present representative qualitative examples in Fig. 5. In the top row, the left videos in each pair exhibit noticeable flickering artifacts and inconsistent motion across frames. While our model accurately reflects the degraded perceptual quality caused by these temporal distortions, *IP-IQA*, the strongest perceptual-quality baseline, fails to capture such inter-frame inconsistencies, confirming our model captures quality beyond spatial appearance. In the bottom example, although the left videos in each pair appear roughly aligned with the prompt, there is a semantic mismatch with the keywords ‘four’ or ‘measure’. Our model precisely identifies the word with weak correspondence, offering fine-grained interpretability. In contrast, *T2VQA*, the most competitive baseline, tends to produce contradictory rankings, lacking fine-grained assessment capability. More qualitative results are provided in the supplementary material.

Moreover, we perform a gMAD (Ma et al., 2018) competition to compare *EduVQA* and *T2VQA* on both perceptual quality and prompt alignment. The gMAD identifies video pairs where one model assigns similar scores while the other produces markedly different predictions, revealing incon-



Figure 5. Qualitative comparison of perceptual quality (top row) and prompt alignment (bottom row). We compare our EduVQA model against state-of-the-art baselines, IP-IQA and T2VQA, in each quality dimensions. In each video pair, the right video exhibits *superior* perceptual quality or prompt alignment compared to the left. EduVQA consistently aligns with human judgments, while IP-IQA and T2VQA produce rankings contrary to the MOS.



Figure 6. gMAD competition results between T2VQA and our EduVQA. Columns 1–2: perceptual quality comparison; Columns 3–4: prompt alignment comparison. zoomed-in view for clarity.

sistencies with human perception. As shown in Fig. 6, we organize the comparisons into two types for each dimension. For perceptual quality (columns 1–2): in column 1, *T2VQA* acts as the defender, assigning similar scores to clips that humans perceive as different, and in column 2, *T2VQA* acts as the attacker, predicting different scores for clips that humans perceive as similar. In both cases, *EduVQA* correctly distinguishes or aligns with human perception, demonstrating its sensitivity to subtle temporal distortions. Similarly, for prompt alignment (columns 3–4), we test the defender and attacker setups: *EduVQA* consistently provides scores that better match human judgments, accurately capturing semantic mismatches that *T2VQA* fails to detect. These results highlight the superior robustness of *EduVQA*.

## 5.6. Ablation Study

We analyze the contribution of each component through an ablation study summarized in Table 3. Starting from a baseline without cross-modality fusion or sub-dimensional supervision (ID 1), introducing the fusion module (ID 2) yields clear gains, confirming the necessity of visual–textual interaction. Adding the spatial–temporal (ST) and word-level (WL) branches (ID 3) further improves both perceptual

and alignment correlations. Removing either ST (ID 4) or WL (ID 5) leads to performance drops in the corresponding dimension, indicating their complementarity. Replacing our specialized MoE with a conventional 1D MoE (ID 6) also degrades performance, demonstrating the advantage of structured 2D expert routing. The full configuration (ID 7) achieves the best overall correlation, validating the effectiveness of jointly modeling fusion, expert learning, and fine-grained supervision.

Table 3. Ablation results on cross-modality fusion, MoE configurations, and fine-grained sub-dimension supervision. “ST” and “WL” denote spatial–temporal perceptual and word-level alignment branches, respectively.

ID	Fusion	MoE			Sub-dim.		Perception		Alignment		
		Vanilla	Per.	Aln.	ST	WL	PLCC	SRCC	PLCC	SRCC	
1	✗	✗	✗	✗	✗	✗	✗	0.845	0.836	0.744	0.737
2	✓	✗	✗	✗	✗	✗	✗	0.863	0.851	0.756	0.750
3	✓	✗	✗	✗	✓	✓	✓	0.869	0.859	0.760	0.751
4	✓	✗	✗	✗	✗	✓	✓	0.860	0.849	0.762	0.754
5	✓	✗	✗	✗	✓	✗	✗	0.873	0.862	0.747	0.741
6	✓	✓	✓	✓	✓	✓	✓	0.874	0.862	0.763	0.754
7	✓	✗	✓	✓	✓	✓	✓	<b>0.879</b>	<b>0.869</b>	<b>0.768</b>	<b>0.757</b>

## 6. Conclusion

We introduce *EduAIGV-1k*, the first benchmark dedicated to assessing the quality of AI-generated educational videos. With fine-grained perceptual and alignment annotations, it enables more reliable and interpretable evaluation of instructional content. Built upon this dataset, our *EduVQA* model employs a structured 2D Mixture-of-Experts (MoE) design to jointly capture spatial–temporal fidelity and word-level alignment. Comprehensive experiments verify its superior capability in detecting critical quality issues in educational AIGVs. We believe this work establishes a solid foundation for future research on quality-aware generation and evaluation in education-oriented AI video systems.

## References

- ByteDance. Dreamina. <https://jimeng.jianying.com/>, 2024. Accessed: 2025-08-01.
- Chen, B., Zhu, L., Li, G., Lu, F., Fan, H., and Wang, S. Learning generalized spatial-temporal deep feature representation for no-reference video quality assessment. *IEEE Transactions on Circuits and Systems for Video Technology*, 32(4):1903–1916, 2021.
- Chen, H., Xia, M., He, Y., Zhang, Y., Cun, X., Yang, S., Xing, J., Liu, Y., Chen, Q., Wang, X., Weng, C., and Shan, Y. Videocrafter1: Open diffusion models for high-quality video generation. 2023a.
- Chen, H., Xia, M., He, Y., Zhang, Y., Cun, X., Yang, S., Xing, J., Liu, Y., Chen, Q., Wang, X., et al. Videocrafter1: Open diffusion models for high-quality video generation. *arXiv preprint arXiv:2310.19512*, 2023b.
- Chen, Z., Sun, W., Tian, Y., Jia, J., Zhang, Z., Jiarui, W., Huang, R., Min, X., Zhai, G., and Zhang, W. Gaia: Rethinking action quality assessment for AI-generated videos. *Neural Information Processing Systems*, 37: 40111–40144, 2024.
- Cheng, X., Zhang, W., Zhang, S., Yang, J., Guan, X., Wu, X., Li, X., Zhang, G., Liu, J., Mai, Y., et al. SimpleVQA: Multimodal factuality evaluation for multimodal large language models. *arXiv preprint arXiv:2502.13059*, 2025.
- Core, C. Common core state standards for mathematics. *Washington, DC*, 2010.
- Deng, K., Fei, T., Huang, X., and Peng, Y. IRC-GAN: introspective recurrent convolutional gan for text-to-video generation. In *International Joint Conference on Artificial Intelligence*, pp. 2216–2222, 2019.
- Esser, P., Chiu, J., Atighehchian, P., Granskog, J., and Geramidis, A. Structure and content-guided video synthesis with diffusion models. In *IEEE/CVF International Conference on Computer Vision*, pp. 7346–7356, 2023.
- Glorot, X., Bordes, A., and Bengio, Y. Deep sparse rectifier neural networks. In *Proceedings of the Fourteenth International Conference on Artificial Intelligence and Statistics*, pp. 315–323. JMLR Workshop and Conference Proceedings, 2011.
- He, Y., Yang, T., Zhang, Y., Shan, Y., and Chen, Q. Latent video diffusion models for high-fidelity video generation with arbitrary lengths. *arXiv preprint arXiv:2211.13221*, 2022.
- Heusel, M., Ramsauer, H., Unterthiner, T., Nessler, B., and Hochreiter, S. GANs trained by a two time-scale update rule converge to a local nash equilibrium. *Neural Information Processing Systems*, 30, 2017.
- Ho, J., Salimans, T., Gritsenko, A., Chan, W., Norouzi, M., and Fleet, D. J. Video diffusion models. *Neural Information Processing Systems*, 35:8633–8646, 2022.
- Hong, W., Ding, M., Zheng, W., Liu, X., and Tang, J. CogVideo: Large-scale pretraining for text-to-video generation via transformers. *arXiv preprint arXiv:2205.15868*, 2022.
- Huang, Z., He, Y., Yu, J., Zhang, F., Si, C., Jiang, Y., Zhang, Y., Wu, T., Jin, Q., Chanpaisit, N., et al. VBench: Comprehensive benchmark suite for video generative models. In *IEEE Conference on Computer Vision and Pattern Recognition*, pp. 21807–21818, 2024.
- Ke, J., Wang, Q., Wang, Y., Milanfar, P., and Yang, F. MUSIQ: Multi-scale image quality transformer. In *IEEE International Conference on Computer Vision*, pp. 5148–5157, 2021.
- Khachatryan, L., Movsisyan, A., Tadevosyan, V., Henschel, R., Wang, Z., Navasardyan, S., and Shi, H. Text2Video-Zero: Text-to-image diffusion models are zero-shot video generators. In *Proceedings of the IEEE/CVF International Conference on Computer Vision (ICCV)*, pp. 15954–15964, 2023.
- Kingma, D. P. and Ba, J. Adam: A method for stochastic optimization. *arXiv preprint arXiv:1412.6980*, 2014.
- Kling AI. Kling AI Platform. <https://app.klingai.com/cn/>, 2024. Accessed: 2025-07-31.
- Kou, T., Liu, X., Zhang, Z., Li, C., Wu, H., Min, X., Zhai, G., and Liu, N. Subjective-aligned dataset and metric for text-to-video quality assessment. In *ACM International Conference on Multimedia*, pp. 7793–7802, 2024a.
- Kou, T., Liu, X., Zhang, Z., Li, C., Wu, H., Min, X., Zhai, G., and Liu, N. Subjective-aligned dataset and metric for text-to-video quality assessment. In *ACM International Conference on Multimedia*, pp. 7793–7802, 2024b.
- Li, B., Zhang, W., Tian, M., Zhai, G., and Wang, X. Blindly assess quality of in-the-wild videos via quality-aware pre-training and motion perception. *IEEE Transactions on Circuits and Systems for Video Technology*, 32(9):5944–5958, 2022a.
- Li, D., Jiang, T., and Jiang, M. Quality assessment of in-the-wild videos. In *Proceedings of the 27th ACM international conference on multimedia*, pp. 2351–2359, 2019.
- Li, J., Li, D., Xiong, C., and Hoi, S. BLIP: Bootstrapping language-image pre-training for unified vision-language understanding and generation. In *International Conference on Machine Learning*, pp. 12888–12900. PMLR, 2022b.

- Li, Y., Min, M., Shen, D., Carlson, D., and Carin, L. Video generation from text. In *AAAI Conference on Artificial Intelligence*, volume 32, 2018.
- Liu, Y., Cun, X., Liu, X., Wang, X., Zhang, Y., Chen, H., Liu, Y., Zeng, T., Chan, R., and Shan, Y. Eval-Crafter: Benchmarking and evaluating large video generation models. In *IEEE Conference on Computer Vision and Pattern Recognition*, pp. 22139–22149, 2024.
- Liu, Z., Ning, J., Cao, Y., Wei, Y., Zhang, Z., Lin, S., and Hu, H. Video Swin Transformer. In *IEEE Conference on Computer Vision and Pattern Recognition*, pp. 3202–3211, 2022.
- Ma, K., Duanmu, Z., Wang, Z., Wu, Q., Liu, W., Yong, H., Li, H., and Zhang, L. Group maximum differentiation competition: Model comparison with few samples. *IEEE Transactions on Pattern Analysis and Machine Intelligence*, 42(4):851–864, 2018.
- Mittal, A., Soundararajan, R., and Bovik, A. C. Making a “completely blind” image quality analyzer. *IEEE Signal Processing Letters*, 20(3):209–212, 2012.
- Mullan, J., Crawbuck, D., and Sastry, A. Hotshot-XL, October 2023. URL <https://github.com/hotshotco/hotshot-xl>.
- Mullis, I. V., Martin, M. O., and von Davier, M. Timss 2023 assessment frameworks. *International Association for the Evaluation of Educational Achievement*, 2021.
- OpenAI. Sora: A text-to-video diffusion model, 2024. <https://openai.com/sora>.
- Peng, F., Fu, H., Ming, A., Wang, C., Ma, H., He, S., Dou, Z., and Chen, S. Aigc image quality assessment via image-prompt correspondence. In *Proceedings of the IEEE/CVF Conference on Computer Vision and Pattern Recognition*, pp. 6432–6441, 2024.
- Qu, B., Li, H., and Gao, W. Bringing textual prompt to ai-generated image quality assessment. In *IEEE International Conference on Multimedia and Expo*, pp. 1–6. IEEE, 2024.
- Radford, A., Kim, J. W., Hallacy, C., Ramesh, A., Goh, G., Agarwal, S., Sastry, G., Askell, A., Mishkin, P., Clark, J., et al. Learning transferable visual models from natural language supervision. In *International Conference on Machine Learning*, pp. 8748–8763, 2021.
- Runway Research. Gen-3 Alpha: A new frontier for creative ai. <https://runwayml.com/blog/gen-3-alpha/>, 2024. Accessed: 2025-08-01.
- Salimans, T., Goodfellow, I., Zaremba, W., Cheung, V., Radford, A., and Chen, X. Improved techniques for training GANs. *Neural Information Processing Systems*, 29, 2016.
- Unterthiner, T., Van Steenkiste, S., Kurach, K., Marinier, R., Michalski, M., and Gelly, S. Towards accurate generative models of video: A new metric & challenges. *arXiv preprint arXiv:1812.01717*, 2018.
- Wang, J., Chan, K. C., and Loy, C. C. Exploring clip for assessing the look and feel of images. In *AAAI conference on artificial intelligence*, volume 37, pp. 2555–2563, 2023.
- Wang, Y., Chen, X., Ma, X., Zhou, S., Huang, Z., Wang, Y., Yang, C., He, Y., Yu, J., Yang, P., et al. LAVIE: High-quality video generation with cascaded latent diffusion models. *International Journal of Computer Vision*, 2024a.
- Wang, Y., Xiong, T., Zhou, D., Lin, Z., Zhao, Y., Kang, B., Feng, J., and Liu, X. Loong: Generating minute-level long videos with autoregressive language models. *arXiv preprint arXiv:2410.02757*, 2024b.
- Weng, Z., Yang, X., Li, A., Wu, Z., and Jiang, Y.-G. Open-VCLIP: Transforming clip to an open-vocabulary video model via interpolated weight optimization. In *International conference on machine learning*, pp. 36978–36989. PMLR, 2023.
- Wu, C., Liang, J., Ji, L., Yang, F., Fang, Y., Jiang, D., and Duan, N. NÜWA: Visual synthesis pre-training for neural visual world creation. In *European Conference on Computer Vision*, pp. 720–736, 2022a.
- Wu, H., Chen, C., Hou, J., Liao, L., Wang, A., Sun, W., Yan, Q., and Lin, W. Fast-VQA: Efficient end-to-end video quality assessment with fragment sampling. In *European conference on computer vision*, pp. 538–554. Springer, 2022b.
- Wu, H., Chen, C., Liao, L., Hou, J., Sun, W., Yan, Q., Gu, J., and Lin, W. Neighbourhood representative sampling for efficient end-to-end video quality assessment. *IEEE Transactions on Pattern Analysis and Machine Intelligence*, 45(12):15185–15202, 2023a.
- Wu, H., Zhang, E., Liao, L., Chen, C., Hou, J., Wang, A., Sun, W., Yan, Q., and Lin, W. Exploring video quality assessment on user generated contents from aesthetic and technical perspectives. In *IEEE International Conference on Computer Vision*, pp. 18681–18691, 2023b.
- Wu, H., Zhang, Z., Zhang, W., Chen, C., Liao, L., Li, C., Gao, Y., Wang, A., Zhang, E., Sun, W., et al. Q-Align: Teaching LMMs for visual scoring via discrete text-defined levels. *arXiv preprint arXiv:2312.17090*, 2023c.

Xing, F., Li, M., Wang, Y.-G., Zhu, G., and Cao, X. Clipvqa: Video quality assessment via clip. *IEEE Transactions on Broadcasting*, 2024.

Xu, J., Liu, X., Wu, Y., Tong, Y., Li, Q., Ding, M., Tang, J., and Dong, Y. ImageReward: Learning and evaluating human preferences for text-to-image generation. *Neural Information Processing Systems*, 36:15903–15935, 2023.

Zhang, D. J., Wu, J. Z., Liu, J.-W., Zhao, R., Ran, L., Gu, Y., Gao, D., and Shou, M. Z. Show-1: Marrying pixel and latent diffusion models for text-to-video generation. *International Journal of Computer Vision*, 133(4):1879–1893, 2025.

Zhang, Z., Li, X., Sun, W., Jia, J., Min, X., Zhang, Z., Li, C., Chen, Z., Wang, P., Ji, Z., Sun, F., Jui, S., and Zhai, G. Benchmarking multi-dimensional aigc video quality assessment: A dataset and unified model. *ACM Transactions on Multimedia Computing, Communications and Applications*, 21:1 – 24, 2024. URL <https://api.semanticscholar.org/CorpusID:271570974>.

## A. Dataset Construction and Analysis

In this section, we provide a detailed overview of our dataset construction, including the prompt generation, subjective annotation and processing, and illustrative examples across different quality dimensions.

### A.1. Prompt Design

Recent advances in text-to-video (T2V) generation have demonstrated remarkable progress, especially in applications such as entertainment, advertising, and creative media. However, in domains requiring highly precise visual semantics, such as mathematics education, existing T2V systems still exhibit significant limitations. In our preliminary experiments, we observed that state-of-the-art T2V models usually struggle to faithfully generate abstract, symbolic, or spatially precise mathematical content. For example, they may fail to illustrate exact counting tasks (e.g., “ten apples appearing sequentially on a table”) or accurately depict spatial transformations (e.g., “a square rotating 45 degrees around its center”). These limitations highlight the challenges of producing pedagogically meaningful visualizations and motivated our careful design of prompts to generate educationally relevant videos.

Through systematic experimentation, we found that grounding mathematical concepts in realistic, everyday scenarios substantially improves T2V generation quality. By anchoring abstract ideas in visually plausible contexts, the models are able to generate coherent videos that faithfully represent core mathematical concepts. Across different T2V architectures, we observed that certain types of concepts, such as simple numerosity and basic geometric arrangements can be reliably generated when paired with concrete scenarios. This observation directly informs our dataset design philosophy: abstract concepts should be visually grounded to be effectively realized in video.

We derive our prompt content from four domains: **Numbers**, **Geometry**, **Measurement**, and **Probability**. We leverage GPT-4o to generate candidate prompts by grounding curriculum-relevant concepts in concrete and visually plausible everyday scenarios. The word cloud distribution is shown in Fig. 7 and the generation details are as follows:

**Numbers.** Counting, number comparison, basic number operations, and basic fractions. Experiments show that models generate small quantities (1–3 objects) reliably, but counts exceeding 5 often lead to errors. Arithmetic operations are represented either through object attributes (e.g., “color, size, or object attributes to imply addition/subtraction”) or object movements (e.g., “leaving or entering” to indicate subtraction/addition”). The former produces more stable and coherent videos, while the latter often causes visual artifacts.

**Geometry.** Shape recognition, shape composition, spatial reasoning, and reasoning about attributes. T2V models are more successful in generating familiar geometric shapes and transformations when grounded in real-world contexts (e.g., “A kite flies in a triangle shape on a sunny day”). In addition to single-shape prompts, our dataset also includes compositional geometric descriptions involving multiple shapes and spatial relations (e.g., “A trophy has a cylindrical base with a star-shaped top”). These prompts impose higher demands on generative models and call for more fine-grained quality evaluation to capture subtle geometric inaccuracies and spatial inconsistencies.

**Measurement.** Measurable attributes and categorical data. Since current T2V models are generally insensitive to fine-grained numerical details such as scales, units, or markings, direct visualization of quantitative measurement is often unreliable. To address this, our dataset constructs contextual measurement and classification scenarios (e.g., “A doctor measures a child height using a stadiometer”), allowing models to express fundamental measurement concepts through realistic actions and familiar objects rather than abstract numbers. Such design not only aligns with early mathematics pedagogy but also facilitates intuitive visual understanding for young learners, bridging the gap between quantitative reasoning and perceptually grounded representations.

**Probability.** Foundations of randomness and chance, including coin flips, dice rolls, and simple stochastic events (e.g., “A driver decides which lane to pick at an intersection with three choices”). Grounding in concrete events enables T2V models to approximate probabilistic outcomes, making abstract probabilistic reasoning more visually interpretable.

From an initial pool, we curate *113 high-quality prompts* via expert filtering, covering four core domains in early mathematics education: *Numbers (43 prompts)*, *Geometry (40 prompts)*, *Measurement (20 prompts)*, and *Probability (10 prompts)*,



## EduVQA: Benchmarking AI-Generated Video Quality Assessment for Education

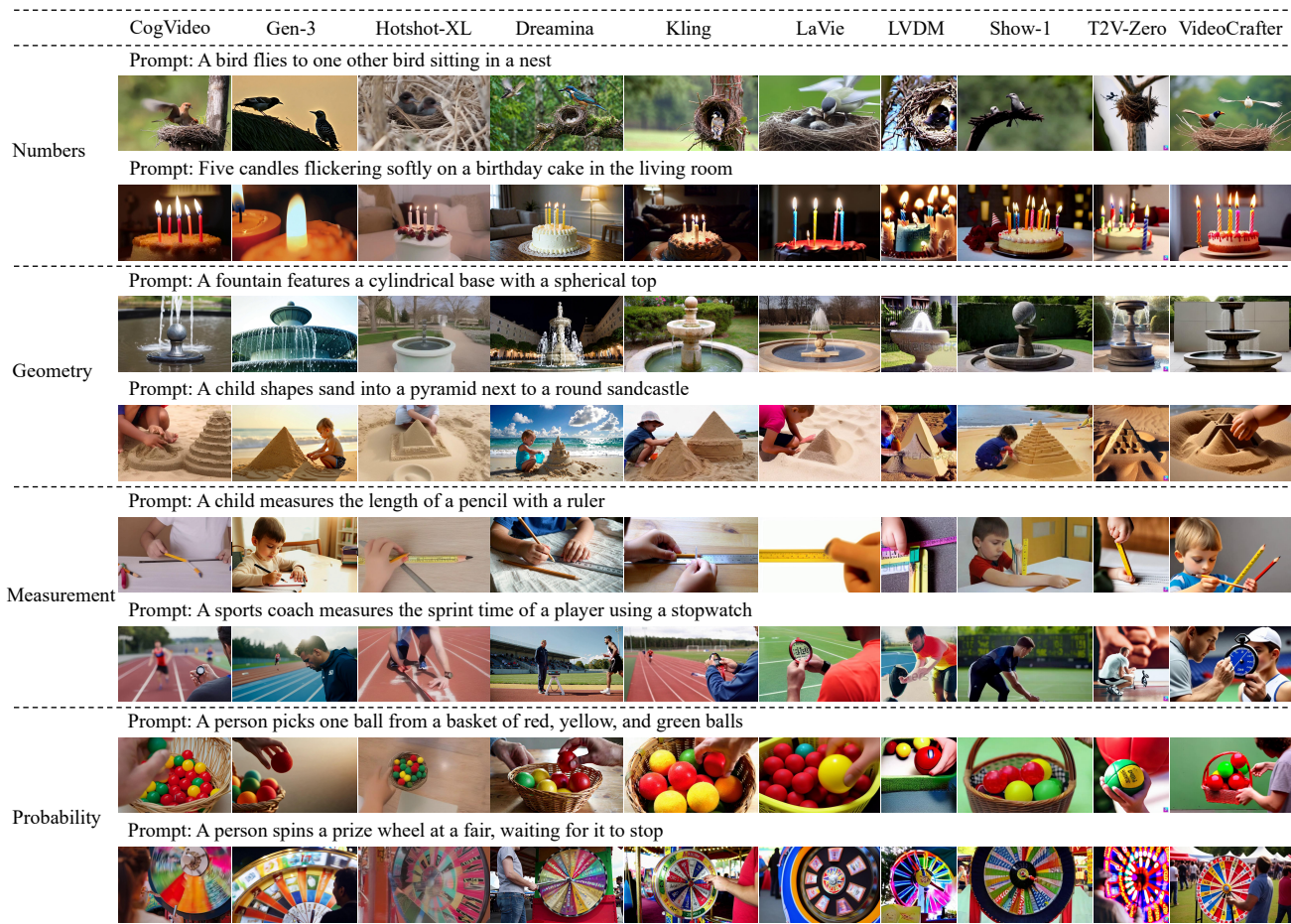


Figure 8. Representative samples from EduAIGV-1K, covering four categories: Numbers, Geometry, Measurement, and Probability.

annotators are excluded from aggregation, since such sparsely evaluated words do not provide reliable consensus. Only tokens with sufficient ratings are retained when computing the final word-level MOS.

### A.3. Representative Samples

We present representative samples from each quality dimension Fig. 10, arranged from high to low levels. The qualitative evidence demonstrates that the dataset captures fine-grained and dimension-specific differences in video quality, providing a solid basis for benchmarking models on multi-dimensional quality understanding and prediction.

## B. Extended Experimental Evaluation

In this section, we present expanded analyses and visualizations that complement the experimental results in the main manuscript, including detailed qualitative comparisons and extended gMAD evaluations.

### B.1. Qualitative Comparisons

In Fig. 11, we present representative samples across multiple quality dimensions to further examine the relationship between model predictions and human judgments. The results demonstrate that our method reliably tracks perceptual degradations and semantic inaccuracies, producing scores that closely align with human assessment across both spatial-temporal fidelity and prompt grounding. Even in challenging scenarios, such as rapid motion, fine-grained scene details, or abstract mathematical instructions, the predicted quality remains stable, interpretable, and consistent with observed subjective trends.

To further validate alignment at a finer granularity, Fig. 11 visualizes the word-level alignment scores predicted by

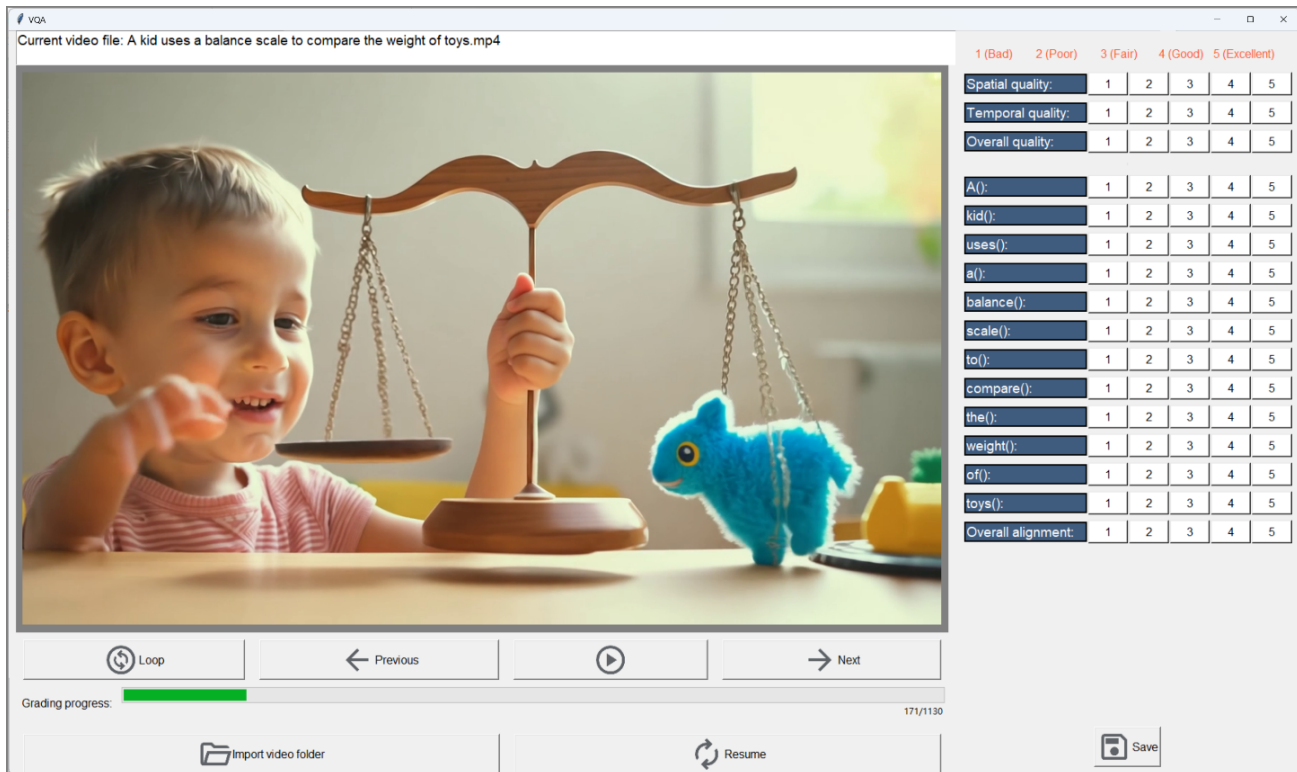


Figure 9. Fine-grained quality annotation interface.

*EduVQA* alongside the corresponding MOS values. The prediction curves exhibit high consistency with human annotations, maintaining similar fluctuation patterns across different instructional keywords. This strong correspondence indicates that the model not only captures global semantic correctness but also effectively reflects concept-level variations relevant to educational video understanding.

## B.2. Extended gMAD Analysis

The main manuscript presents preliminary gMAD comparisons illustrating performance differences between *EduVQA* and *T2VQA* in perceptual assessment and prompt alignment. Due to space constraints, only a limited subset of examples could be included. The supplementary material provides a more comprehensive collection of gMAD visualizations (see Fig. 12), enabling a fuller examination of model behavior under adversarial comparison. These extended results demonstrate improved robustness, clearer discrimination in challenging cases, and enhanced interpretability of *EduVQA* within the gMAD evaluation framework.

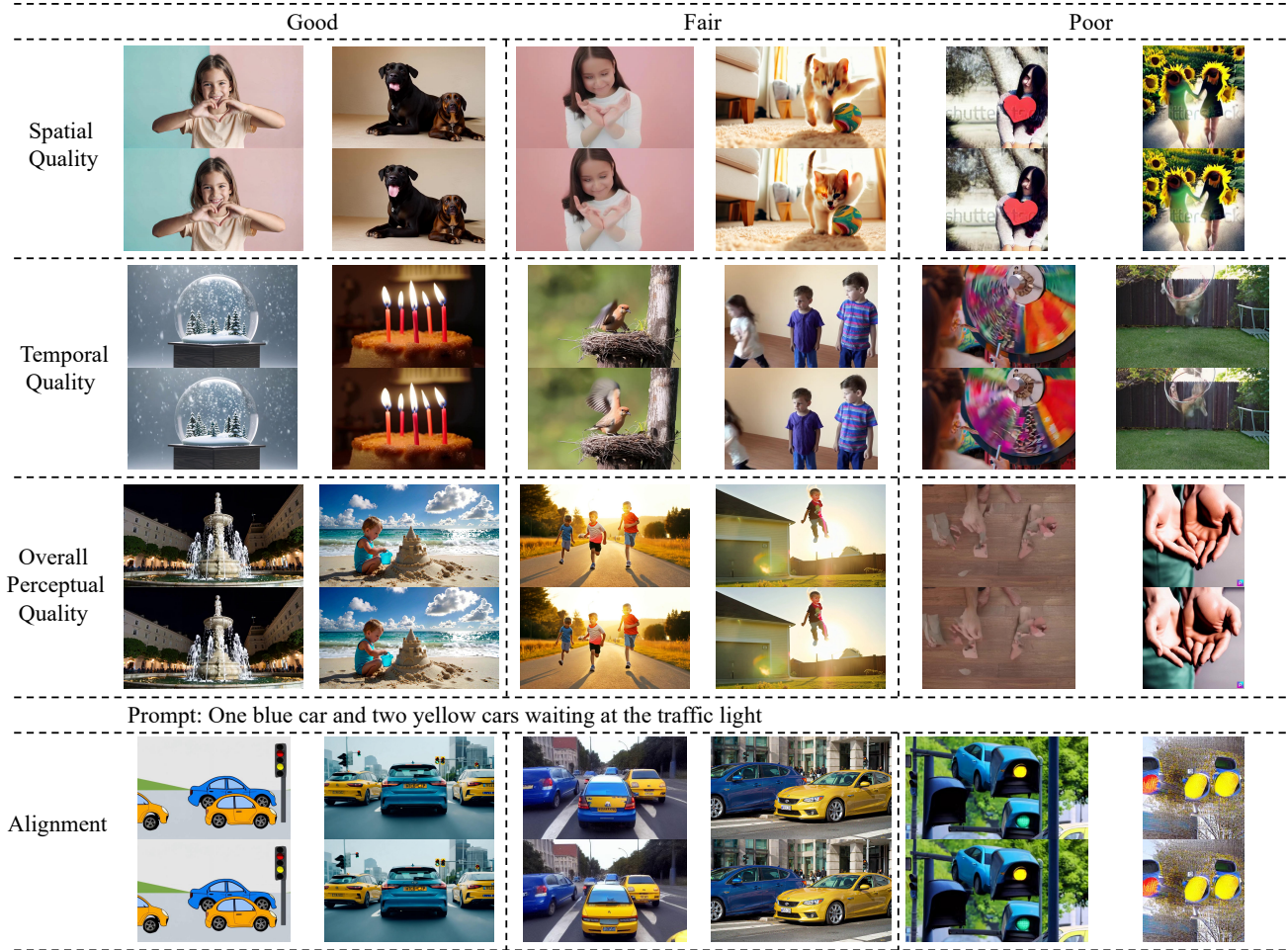
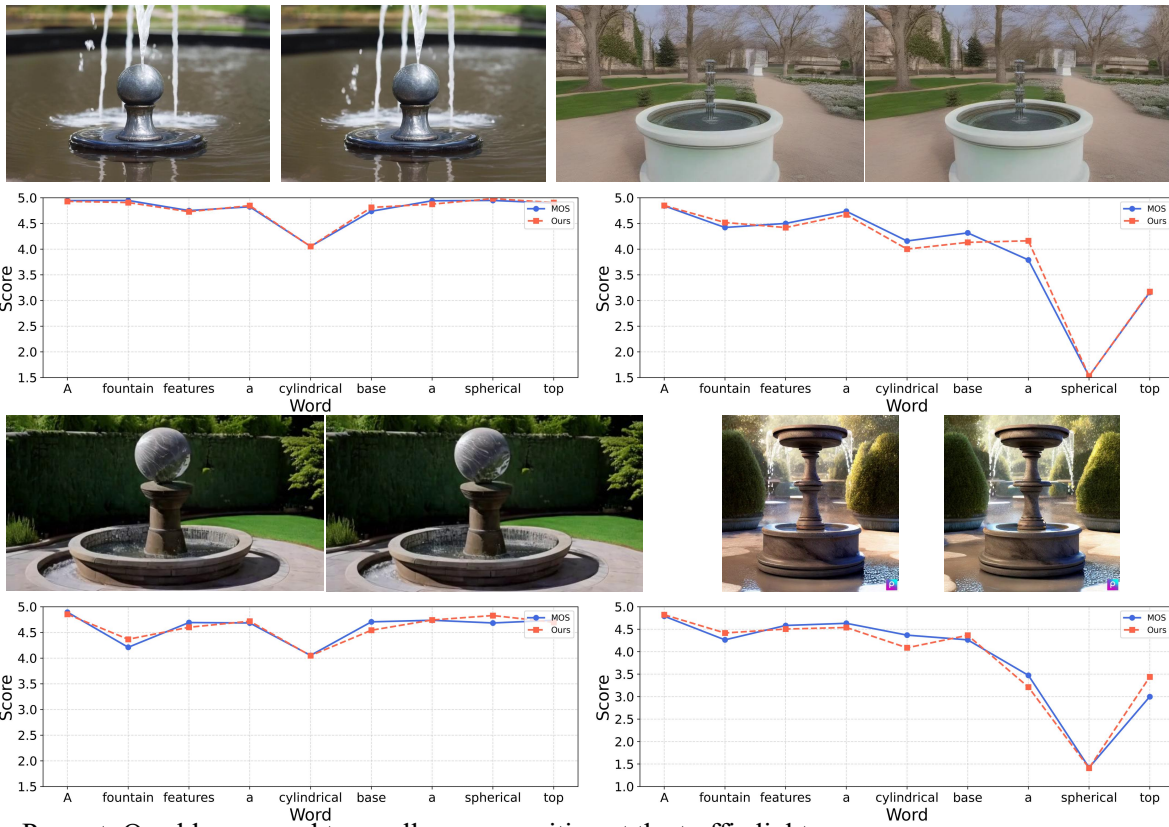


Figure 10. Qualitative examples across different quality dimensions. From left to right: good-, fair-, and low-quality samples in spatial, temporal, overall perceptual, and, alignment dimensions.



Figure 11. Comparison between predicted scores and MOS across multiple quality dimensions and quality levels.

Prompt: A fountain features a cylindrical base with a spherical top



Prompt: One blue car and two yellow cars waiting at the traffic light

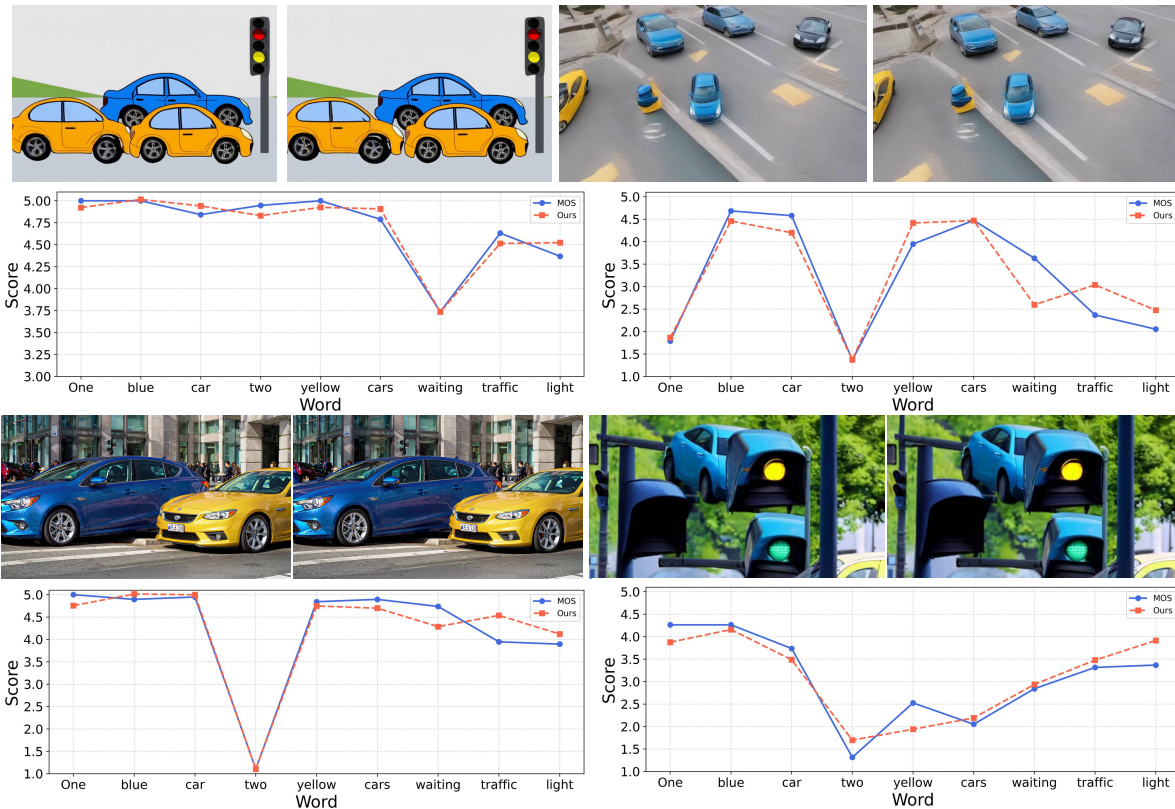


Figure 11. Word-level alignment prediction curves compared with MOS annotations.

EduVQA: Benchmarking AI-Generated Video Quality Assessment for Education

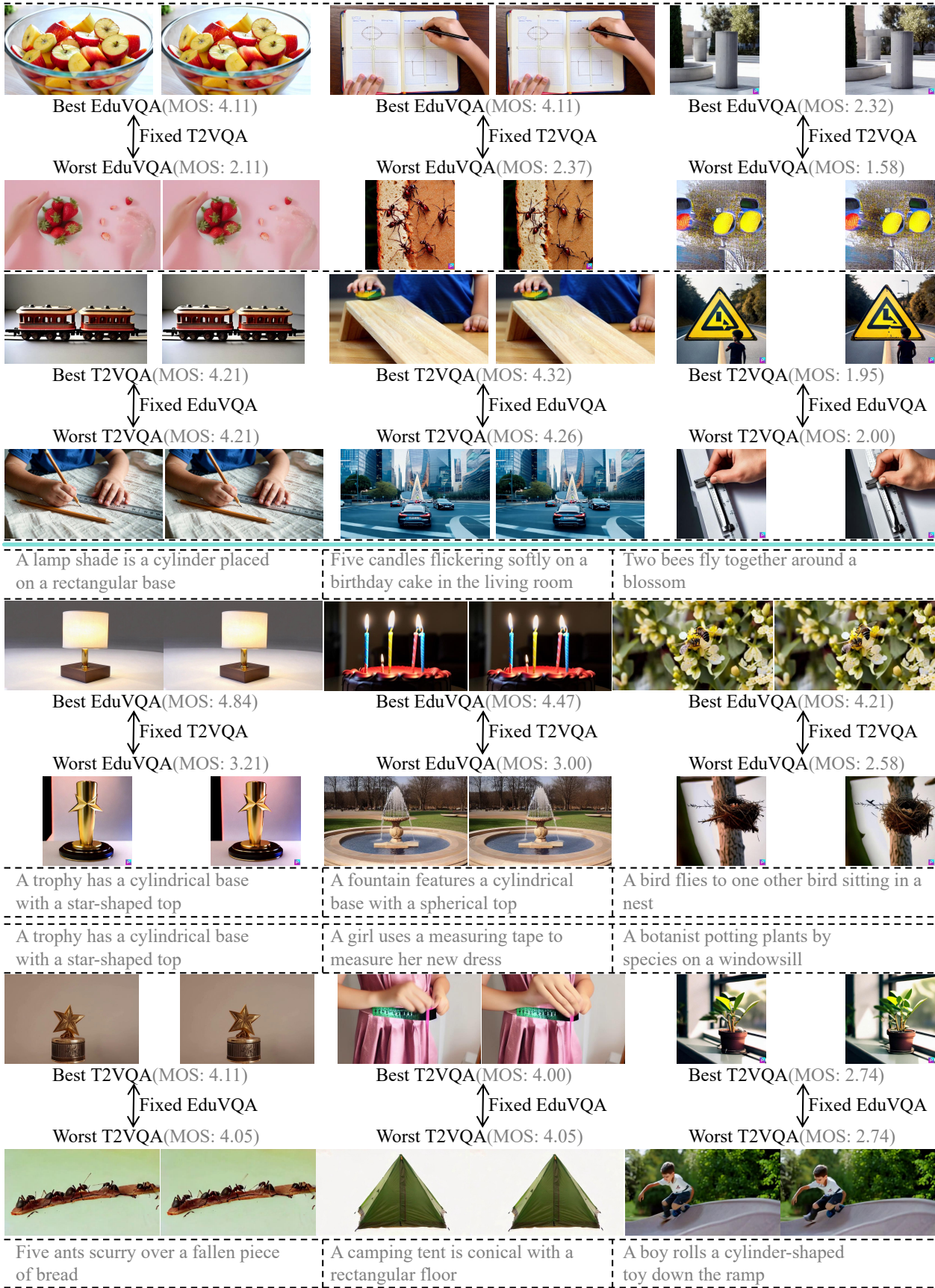


Figure 12. gMAD competition results between T2VQA and our EduVQA. Rows 1–2: perceptual quality comparison; Rows 3–4: prompt alignment comparison.